



Archived at the Flinders Academic Commons:

<http://dspace.flinders.edu.au/dspace/>

The following article appeared as:

Kato, H., Masui, H., Hoshino, M., Cho, H., Ingolfsson, O., Brunger, M.J., Limao-Vieira, P. and Tanaka, H., 2010. A-band methyl halide dissociation via electronic curve crossing as studied by electron energy loss spectroscopy. *Journal of Chemical Physics*, 133, 054304.

and may be found at:

http://jcp.aip.org/resource/1/jcpsa6/v133/i5/p054304_s1

DOI: <http://dx.doi.org/10.1063/1.3464483>

Copyright (2010) American Institute of Physics. This article may be downloaded for personal use only. Any other use requires prior permission of the authors and the American Institute of Physics.

A-band methyl halide dissociation via electronic curve crossing as studied by electron energy loss spectroscopy

H. Kato, H. Masui, M. Hoshino, H. Cho, O. Ingólfsson et al.

Citation: *J. Chem. Phys.* **133**, 054304 (2010); doi: 10.1063/1.3464483

View online: <http://dx.doi.org/10.1063/1.3464483>

View Table of Contents: <http://jcp.aip.org/resource/1/JCPSA6/v133/i5>

Published by the [American Institute of Physics](#).

Additional information on *J. Chem. Phys.*

Journal Homepage: <http://jcp.aip.org/>

Journal Information: http://jcp.aip.org/about/about_the_journal

Top downloads: http://jcp.aip.org/features/most_downloaded

Information for Authors: <http://jcp.aip.org/authors>

ADVERTISEMENT



Goodfellow
metals • ceramics • polymers • composites
70,000 products
450 different materials
small quantities fast

www.goodfellowusa.com

A-band methyl halide dissociation via electronic curve crossing as studied by electron energy loss spectroscopy

H. Kato,¹ H. Masui,¹ M. Hoshino,¹ H. Cho,² O. Ingólfsson,³ M. J. Brunger,⁴ P. Limão-Vieira,^{1,5,a)} and H. Tanaka¹

¹Department of Physics, Sophia University, Tokyo 102-8554, Japan

²Department of Physics, Chungnam National University, Daejeon 305-764, Republic of Korea

³Department of Chemistry, University of Iceland, Science Institute, Reykjavík 107, Iceland

⁴ARC Centre for Antimatter-Matter Studies, Flinders University, G.P.O. Box 2100, Adelaide, South Australia 5001, Australia

⁵Departamento de Física, Laboratório de Colisões Atômicas e Moleculares, CEFITEC, FCT, Universidade Nova de Lisboa, 2829-516 Caparica, Portugal

(Received 17 May 2010; accepted 21 June 2010; published online 3 August 2010)

Excitation of the A-band low-lying electronic states in the methyl halides, CH₃I, CH₃Br, CH₃Cl, and CH₃F, has been investigated for the ($n \rightarrow \sigma^*$) transitions, using electron energy loss spectroscopy (EELS) in the range of 3.5–7.5 eV. For the methyl halides, CH₃I, CH₃Br, and CH₃Cl, three components of the Q complex (³ Q_1 , ³ Q_0 , and ¹ Q_1) were directly observed, with the exception of methyl fluoride, in the optically forbidden EELS experimental conditions of this investigation. The effect of electronic-state curve crossing emerged in the transition probabilities for the ³ Q_0 and ¹ Q_1 states, with spin-orbit splitting observed and quantified against results from recent *ab initio* studies. © 2010 American Institute of Physics. [doi:10.1063/1.3464483]

I. INTRODUCTION

In this paper we report results from our third and final study into the scattering dynamics for electron collisions from the methyl halides (CH₃X; X=F, Cl, Br, and I). Our first paper¹ dealt with a comprehensive study into elastic electron scattering from these molecules, both theoretical and experimental, while our second contribution addressed resonance phenomena in the behavior of some of their vibrational excitation functions.² Here, we conclude by examining electron impact excitation of the A-band low-lying electronic states in each of these species.

The electronic energies and structures of the methyl halides have been experimentally and theoretically studied for decades (see, e.g. Refs. 1 and 2 and references therein), in particular because (1) they are important compounds in the chemistry of the earth's atmosphere; (2) they may be used in several industrial applications such as the chemical industry in semiconductor etching, low-boiling solvents, as fire extinguishers and in pesticide production; (3) of their relevance in characterizing the behavior of negative ion states in terms of dictating the vibrational excitation and dissociative electron attachment cross sections under electron impact; and (4) the electronic state electron energy loss spectroscopy (EELS) spectra of a similar set of molecules, differing only in the bonded halogen atom, provides useful information on the initial electronic excitation and subsequent inter-surface dynamics. This latter reason is particularly relevant when addressing curve crossing, as we do later in Sec. III.

The vacuum ultraviolet (vuv) absorption spectra of the chloromethanes have been studied by Russell and

co-workers,³ and more recently Eden *et al.*⁴ reported absolute values from high-resolution photoabsorption spectra of CH₃Cl and CH₃I in the energy range of 3.9–10.8 eV (320–115 nm). In that latter work special attention was made to provide a systematic assignment of the spectral features. The vapor phase vuv spectra of the bromomethanes by Causley and Russell⁵ showed that for the A-band, in this absorption region, several overlapping electronic states appear with the degree of their contribution increasing with the number of substituted bromine atoms. EELS data from Nachtigallova *et al.*,⁶ on the low-lying excited states of CH₃Cl, have been compared with results from *ab initio* calculations and the experimental energy difference between the triplet-singlet ($n \rightarrow \sigma^*$) states was found to be 0.4 eV.

Theoretical calculations on the intensities in molecular electronic spectra have been addressed by Mulliken,⁷ with particular attention to the $N \rightarrow Q$ perpendicular type complex arising from the excitation of a nonbonding $np\pi$ halogen electron to a σ^* molecular orbital. Since the 1970s measurements using circular dichroism have provided a large body of information over a wide range of wavelengths for photoabsorption spectroscopy. In particular magnetic circular dichroism (MCD) has allowed resolution of some overlapping transitions in halogen containing molecules including the methyl halides, CH₃I, CH₃Br, and CH₃Cl.⁸ However Gedanken's MCD assignments for the ³ Q_1 , ³ Q_0 , and ¹ Q_1 states, as being the only components of the Q complex, were not definitive as it was not easy to fully resolve them due to a superposition of a negative B-band and a positive A-band signal. Note that an A-band in a MCD spectrum means a derivative line shape due to a transition from the ground state to a degenerate excited state, which is related to the first order Zeeman effect on the upper degenerate state, whereas a B-band is

^{a)}Author to whom correspondence should be addressed. Electronic mail: plimaovieira@fct.unl.pt.

caused by a second order Zeeman effect where two excited states are mixed in the presence of the magnetic field. Moreover, from photofragmentation measurements, it has been well established that accessing 3Q_0 leads to a dissociative state with formation of an $X^*(^2P_{1/2})$ excited halogen atom, while the 1Q_1 and 3Q_1 states lead to $X(^2P_{3/2})$ ground state halogen atoms.

More recently, Ajitha *et al.*⁹ performed experimental studies on electronic curve crossing in the low-lying ($n \rightarrow \sigma^*$) photodissociation dynamics of the alkyl halides together with spin-orbit *ab initio* calculations. Their results have shown that the photodissociation dynamics are driven by the crossing of the excited state surfaces, potential energy curves along the H_3C-X reaction coordinate having been computed to verify that. At about the same time, Townsend *et al.*¹⁰ employed (2+1) REMPI (Resonance Enhanced Multi Photon Ionization) photodissociation with CH_3Cl at 193.3 nm, and concluded that a transition from the ground to the 1Q_1 state contributes predominantly to the A-band profile. Previously Van Veen *et al.*¹¹ used time-of-flight and angular distributions of the CH_3 fragments, from CH_3Br photodissociation in the A-band, and showed no effective adiabatic curve crossing between the 3Q_0 and 1Q_1 states. *Ab initio* potential energy surface and trajectory studies of the A-band photodissociation dynamics of CH_3I , have shown that although the ($n \rightarrow \sigma^*$) transition is mainly governed by the 3Q_0 state, it has a non-negligible 1Q_1 and 3Q_1 state character.^{12,13} This result is in agreement with the zero kinetic energy photoelectron spectroscopy experiment of Strobel *et al.*¹⁴

In this paper we focus our attention on the low-lying excited states of the methyl halides, specifically the A-band corresponding to the ($n \rightarrow \sigma^*$) transition. We assign structures fitted in our EELS measurements to the three underlying electronic states, 3Q_1 , 3Q_0 , and 1Q_1 , and we also discuss the temporary occupation of the 2A_1 repulsive $\sigma^*(C-X)$ ground state of the anions.

II. EXPERIMENTAL

The electron spectrometer used in the present work has been described in detail elsewhere.¹⁵ Briefly, a monochromatic electron beam is generated with a hemispherical electron monochromator and crossed at right angles with an effusive molecular beam that enters the interaction region through a 5 mm long capillary with a 0.3 mm inner diameter. After the electron interaction with the target gas the scattered electrons are detected with a hemispherical electron analyzer. Both the electron monochromator and the energy analyzer are enclosed in separate, differentially pumped housings. The typical base pressure in the main chamber was 2.0×10^{-5} Pa and upon gas admission (CH_3X ; $X=F, Cl, Br$, and I) increased to a pressure of 2.0×10^{-4} Pa.

In the current experiments the energy resolution of the incident electron beam was about 25–35 meV [full width at half maximum (FWHM)], with incident electron currents of a few nanoamperes (depending on the initial electron energy). The incident electron energy was calibrated with respect to the 19.365 eV, 2S resonance in He (Ref. 16) and with respect to the $^2\Pi_g$ resonance in N_2 for the vibrational exci-

tations around 2.4 eV.¹⁷ The hemispherical electron analyzer is placed on a turntable stage and can be rotated from -10° to $+130^\circ$, with respect to the incident electron beam, with an angular resolution of about 1.5° (FWHM). This is obtained through He 2^1P state used to set the zero degree scattering angle with the angular ambiguity which is estimated by the geometrical condition of the acceptance view cone angle of the analyzer together with the mechanical angular-allowance included for the angular rotation.

For the energy loss measurements both the electron energy of the incident beam and the angle of the analyzer were fixed, with the intensity of the scattered electron signal being measured “in sync” with the energy loss. For the lower incident electron energies, it is important to establish the transmission of the analyzer over our energy loss range. Here, an estimate is made through a comparison with the energy dependence of other well known measured cross sections for inelastic scattering. Specifically in the present case we have made use of the helium 2^1P transition. The energy dependence of 2^1P to the elastic intensity ratio in helium at 20° was measured, and compared with well-known values.^{18–20} After consideration of other experimental parameters, the difference between the measured and standard ratios was considered to be a reasonable indicator of the apparatus transmission function. This transmission function was then used when needed to correct the measured EELS spectra.

In this study two approaches were used to obtain absolute differential cross sections (DCSs) for electronic excitation of the CH_3X molecules. In the first method, the absolute scales were obtained by the relative flow technique²¹ using the theoretical elastic cross sections of helium.²² Note that this normalization method was used for scattering angles larger than 10° , where one can easily detect the elastically scattered electrons. For angles smaller than 10° , where the elastic signal to noise becomes problematic, a second normalization technique was used to measure the intensity ratio for electronic excitation of the targets relative to the excitation of the 2^1P state in helium. The 2^1P state DCS,¹⁸ could then be employed to fix the corresponding absolute scales of the electronic excitations in the EELS.

The target molecule, CH_3F , was obtained from PCR Inc. (Gainesville, FL, USA) with a stated purity of 99%, CH_3Cl from Tri Chemical Laboratories Inc. (Yamanashi, Japan) with 99.999% stated purity, CH_3Br from Tokyo Chemical Industry Co. Inc. (Tokyo, Japan) with 99% stated purity and CH_3I from Wako Pure Chemical Industries Ltd (Osaka, Japan) with 95% stated purity.

III. RESULTS AND DISCUSSION

According to Mulliken,⁷ the ground state configuration of the methyl halides is $N: \sigma^2 \pi_x^4: ^1A_1$, where π_x is a $np\pi$ atomic orbital on the halogen and σ the C–X bonding orbital. He also noted that the lowest excited configurations can be represented as $^3,1Q: \sigma^2 \pi_x^3 \sigma^*: ^3,1E$, and that all the methyl halide molecules have C_{3v} symmetry in their electronic ground states. The valence shell molecular orbital configuration of CH_3Cl , CH_3Br , and CH_3I in the electronic ground state can also be represented as

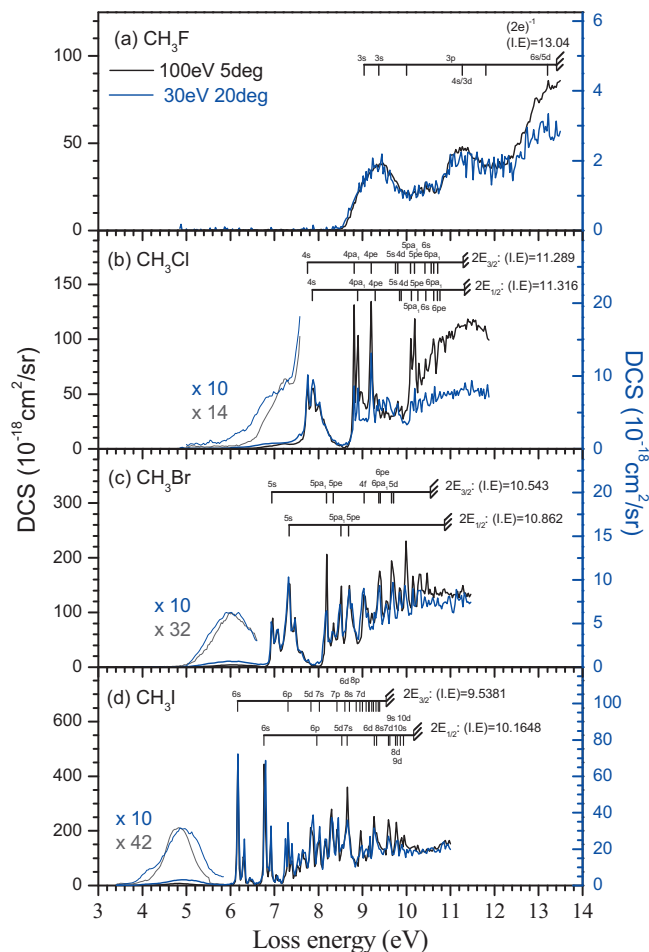


FIG. 1. EELS in the range of 3.0–14 eV for CH_3X : (a) CH_3F , (b) CH_3Cl , (c) CH_3Br , and (d) CH_3I . The elastic peak was also measured at the 20° scattering angle, but has been suppressed here to aid visualization of the electronic-state spectra.

$(1a_1)^2(2a_1)^2(1e)^4(3a_1)^2(2e)^4$: 1A_1 ,^{23–25} whereas for CH_3F it is $(1e)^4(5a_1)^2(2e)^4$: 1A_1 .²⁶ In the ground state of all the CH_3X molecules the highest occupied molecular orbital (HOMO) is the degenerate $2e$ halogen lone pair orbital (n_X). The diffuse feature assigned to the excitation of an electron from the HOMO to the lowest unoccupied molecular orbital of C-X σ^* antibonding character, is the well-established A-band of the methyl halides.^{7,27} This transition potentially results in a prompt dissociation along the C-X bond due to the strong repulsive nature of the excited state. Excitations from the ground state yield a 3Q_0 state with parallel transition and 3Q_1 and 1Q_1 states, with perpendicular character.

Figures 1(a)–1(d) show the EELS for CH_3F , CH_3Cl , CH_3Br , and CH_3I , for 100 and 30 eV incident electrons at scattering angles of 5° and 20° , respectively. The spectra were measured with an energy resolution of 25–35 meV in the energy loss range from 3 eV to at least 11 eV. With the exception of CH_3F , the features corresponding to the excitation of the A-band in the 6.0–7.5, 4.5–6.5, and 3.5–5.5 eV energy loss regions of CH_3Cl , CH_3Br , and CH_3I , respectively, are shown in Figs. 2(a)–2(c). Figure 2 shows expanded views of the low-lying excited bands, where the DCS have been fitted with three Gaussian profile curves in order to resolve the three dipole allowed 3Q_1 , 3Q_0 , and 1Q_1 com-

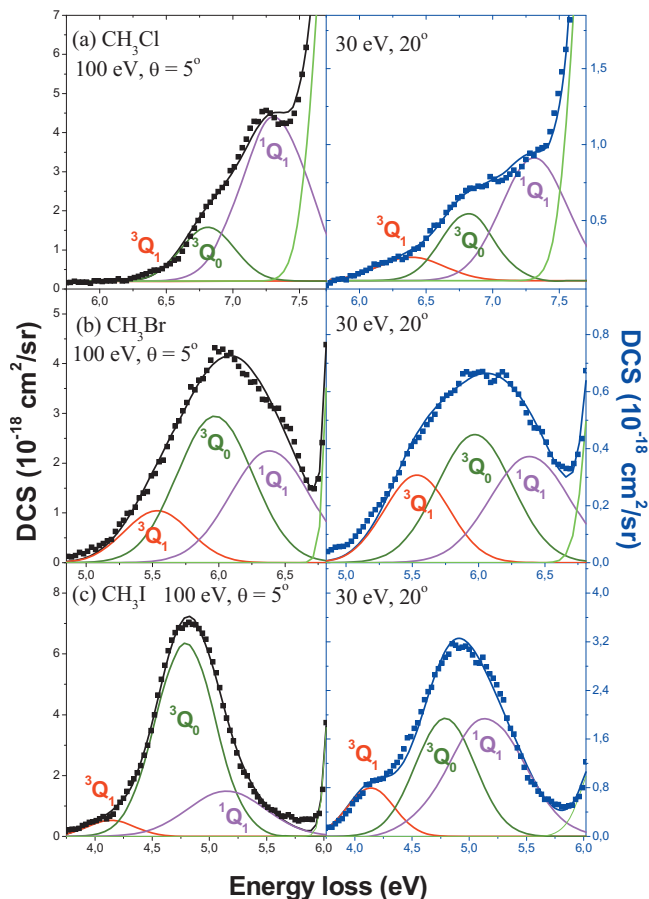


FIG. 2. Gaussian fitting profiles for the Q complex levels of the A-band EELS in (a) CH_3Cl , (b) CH_3Br , and (c) CH_3I .

ponents of the Q complex. Note that in C_{3v} symmetry this corresponds to the $2E$, $2A_1$, and $3E$ states, respectively.

Of particular interest from a detailed analysis of Fig. 1 is the fact that the lowest band maximum is shifted progressively to higher energies in the sequence order $\text{CH}_3\text{F} > \text{CH}_3\text{Cl} > \text{CH}_3\text{Br} > \text{CH}_3\text{I}$, where it becomes increasingly overlapped with the B-band. This is particularly the case for CH_3F . We will now discuss in turn our results for each of the methyl halides in the following sections. Any comparisons drawn between the different halomethanes in the sections below, regarding the intensity of the Q components, will be made for the same incident electron energy and scattering angle conditions, due to the different order of magnitude of the measured DCSs.

A. CH_3I

Mulliken's analysis for intensities in the molecular spectra of the halomethanes (including those reported here), from lower to higher energy loss, predicted a very weak transition assigned to ${}^1A_1 \rightarrow {}^3Q_1$ followed by the strongest transition due to ${}^1A_1 \rightarrow {}^3Q_0$. He also predicted a weak feature assigned to the ${}^1A_1 \rightarrow {}^1Q_1$ transition, which might be somewhat obscured by the more intense feature.⁷ This is generally consistent with our experimental electron energy loss data [Fig. 2(c)], where the ${}^1A_1 \rightarrow {}^3Q_0$ transition dominates at 100 eV impact energies and 5° scattering angle, but the 3Q_1 and 1Q_1 states which are of perpendicular character become more sig-

TABLE I. Vertical excitation energies (values in eV) for the Q states in CH_3I , CH_3Br and CH_3Cl . Where possible the present results are compared against those from previous studies (Refs. 8–10 and 12).

CH_3X	Assignment	Q states			Spin-orbit gap
		$^3Q_1 (\perp)$	$^3Q_0 (\parallel)$	$^1Q_1 (\perp)$	$^1Q_1 - ^3Q_0$
CH_3I	This work	4.14	4.75	5.17	0.42
	Ref. 8	4.14	4.75	5.17	0.42
	Ref. 9 ^a	4.38	4.83	5.05	0.22
	Ref. 9 ^b	4.30	4.69	5.03	0.34
	Ref. 12 ^c	4.629	5.089	5.450	0.361
CH_3Br	This work	5.53 ± 0.06	5.97 ± 0.06	6.37 ± 0.06	0.40 ± 0.08
	Ref. 8	5.33	5.82	6.14	0.32
	Ref. 9 ^b	...	5.73	6.09	0.36
CH_3Cl	This work	6.39 ± 0.06	6.81 ± 0.06	7.31 ± 0.06	0.50 ± 0.08
	Ref. 8	6.57	6.76	7.07	0.31
	Ref. 9 ^b	...	6.36	6.86	0.50
	Ref. 10	0.11

^aAt the MS-CASPT2 level.^bAt the SO-MCQDPT level.^cAdiabatic values.

nificant at an impact energy of 30 eV and 20° scattering angle. Moreover, Mulliken also reported that the tail of the continuum band, toward lower energies, contains evidence for a small fraction of molecules dissociating into the iodine ground state, $I(^2P_{3/2})$, which is not so evident for the analogue bromide (see below).

The three components of the Q complex have been assigned by Gedanken and Rowe⁸ on the basis of their MCD experiments and generally speaking in good agreement with the calculations of Johnson and Kinsey.²⁸ Gedanken and Rowe experimental values are listed in Table I and compared with corresponding results from the present EELS data, where excellent agreement is observed. Comparisons made by these authors on their MCD spectra of CH_3I , CH_3Br , and CH_3Cl , revealed that transitions to 3Q_1 and 3Q_0 become weaker for the last two methyl halides. Our DCS intensities also follow this trend and indeed our data for the 3Q_1 component transition is almost absent for CH_3Cl at a collision energy of 100 eV and a scattering angle of 5°. This behavior is a mirror of the expected spin-orbit coupling that becomes weaker in the sequence $\text{I} > \text{Br} > \text{Cl}$, therefore causing a considerable decrease in the intensity of singlet-triplet transitions when compared to those of a singlet-singlet nature. It is worth noting that our EELS at low impact energy and relatively high scattering angle enhance the singlet to triplet transitions to the detriment of the singlet to singlet transitions [see Figs. 2(a)–2(c)].

From the present CH_3I DCS data at 100 eV, 5° [Fig. 2(a)], the 3Q_0 transition carries about 76% of the continuum intensity, the 1Q_1 transition around 21%, and the 3Q_1 transition has only about 3% of the total intensity. At ~ 4.8 eV (260 nm) most of the 3Q_0 intensity is correlated ($\sim 90\%$) with the $\text{CH}_3 + I(^2P_{1/2})$ dissociative channel. However, a small fraction may also end up in the $\text{CH}_3 + I(^2P_{3/2})$ channel. Our observed intensity values for the 3Q_0 , 1Q_1 , and 3Q_1 transitions are in good agreement with those from the MCD data

of Gedanken and Rowe.⁸ Such behavior may be rationalized in terms of an effective curve crossing between the main states involved, i.e., 3Q_0 and 1Q_1 . Although initial excitation in CH_3I is mainly through the 3Q_0 state, through curve crossing, due to a Landau–Zener type transition (see also discussion for CH_3Br below), the 1Q_1 state becomes relevant at a large nuclear distance yielding the $^2P_{3/2}$ channel.

In the Franck–Condon region, the main transition from the ground state is to the potential energy curve of the 3Q_0 excited state [Fig. 2(c), 100 eV, 5°]. However as the amplitude of the molecular wave function progressively evolves towards the 1Q_1 surface, as the molecule dissociates through a curve crossing, the steepness of 1Q_1 is markedly accentuated along both the radial (C–I) coordinate and the off-axis distortion coordinate, φ ,^{10,12,14} resulting in prompt dissociation. In addition Townsend *et al.*¹⁰ have pointed out that due to the highly repulsive nature of this state, dissociation through 1Q_1 happens more rapidly, sampling a smaller number of distorted geometries than in the 3Q_0 pathway. Therefore, the probability for curve crossing, which is dependent upon distortion away from the C_{3v} symmetry, is expected to be smaller in 1Q_1 than in 3Q_0 . This seems to be consistent with the profile obtained for CH_3I in Fig. 2(c) at an incident energy of 30 eV and 20° scattering angle, where the 1Q_1 perpendicular transition becomes more prominent. This is also reinforced by the polarized emission spectroscopy of Lao *et al.*²⁹ at 4.66 eV (266 nm), who reported a gradual increase in emission from the 1Q_1 potential energy surface on the nv_3 overtones. This is also in agreement with the recent reported resonant feature of CH_3I at 4.7 eV, in the vibrational excitation DCS of Kato *et al.*² Nevertheless, Strobel *et al.*¹⁴ have indicated an increasing relevance of the coupling with a longer evolution time of the wave packet on the potential energy surface.

The branching ratio, $I^*/(I+I^*)$, for the present electron spectroscopy data at around an energy loss of 4.6 eV, yielded

a value ~ 0.76 . This is in very good agreement with the value of ~ 0.80 from the photolysis experiment of Gedanken and Rowe⁸ at 4.66 eV (266 nm), and also with the value of 0.72 obtained from the theoretical predictions of Amatatsu *et al.*¹³

B. CH₃Br

Comparing the shapes of the DCSs for CH₃Br with CH₃I suggests that the Q state potential energy curves are much steeper for the latter than the former. This in turn suggests that the separation for the three Q components in CH₃Br is not so evident, leading to a broader overlap among them. That assertion is clearly visible from the EELS spectra at 100 eV, 5° [Fig. 2(b)]. Such a result is also particularly interesting because the dipole polarizability of the methyl halides follows the sequence CH₃I > CH₃Br > CH₃Cl > CH₃F.¹

The anisotropy parameters measured in the photodissociation studies of Van Veen *et al.*¹¹ indicate that most of the intensity at 5.59 eV (222 nm) is associated with the $^1A_1 \rightarrow ^3Q_0$ and the $^1A_1 \rightarrow ^3Q_1$ transitions, whereas at 6.42 eV (193 nm) the 1Q_1 and 3Q_0 states are mainly excited. Our electron spectroscopy results for these energy values are consistent with those findings [see Fig. 2(b)]. Van Veen *et al.*,¹¹ by assuming identical potential energy curves, noted that the difference arising in the A-band broadening of the bromide (~ 1.0 eV), in comparison to iodide (~ 0.5 eV), is mainly due to the smaller C–X bond for CH₃Br (1.939 Å) relative to that for CH₃I (2.139 Å). This may explain why the maximum absorption for CH₃Br occurs at a larger excitation energy, even though there is a broadening of its absorption width. However we must not discard the fact that for any transition in the Franck–Condon region, the CH₃Br 1Q_1 excited state potential energy curve may be steeper than that for 3Q_0 , as was the case for CH₃I along the (C–I) and distortion coordinates,¹⁰ resulting in prompt dissociation along the former surface and causing a smaller sampling range of distorted geometries than in the latter. Therefore, the probability of a curve crossing appears to be smaller for 1Q_1 in CH₃Br as compared to CH₃I. Recent theoretical studies of the photodissociation dynamics of CH₃Br A-band, using a wave packet propagation technique on coupled *ab initio* potential energy curves, have shown that nonadiabatic population transfers between the 3Q_0 and 1Q_1 states at the conical intersection are small.³⁰ This is in good agreement with the EELS data in Fig. 2(b), where the intensities for 3Q_0 and 1Q_1 remain almost the same in spite of the different impact energies and scattering angles. This has also been observed in the bromine angular distributions, where the ground state Br($^2P_{3/2}$) fragments display predominantly perpendicular behavior across much of the absorption region.¹⁰

Time-of-flight mass spectra with polarized light from Van Veen *et al.*,¹¹ have shown that the Br and Br* fractions formed from the perpendicular and parallel transition, were in agreement with their angular distribution measurements, resulting in a conclusion that curve crossing did not play a significant role for the case of methyl bromide. In addition to the photofragmentation studies, Van Veen *et al.*¹¹ utilized the Landau–Zener model to try and explain the differences in the

effectiveness of curve crossing between the 3Q_0 and 1Q_1 states in CH₃I compared to CH₃Br. The probabilities for an adiabatic transition at the crossing were discussed on the basis of the spin-orbit coupling and the radial velocity, v , with values of 0.30 and 0.06 for CH₃I and CH₃Br, respectively. Therefore these results suggest that such an adiabatic transition may account for the CH₃I experimental observations.

The current relative integral intensities of the 3Q_1 , 3Q_0 , and 1Q_1 states are 14.5%, 47.3%, and 38.2%, respectively, in good agreement with the cross sectional data yield of 11%, 45%, and 44% reported from Van Veen *et al.*¹¹

C. CH₃Cl

Townsend *et al.*¹⁰ obtained energy- and angle-resolved distributions for ground state Cl($^2P_{3/2}$) and spin-orbit excited Cl*($^2P_{1/2}$) photofragments in the A-band of CH₃Cl at 6.42 eV (193.3 nm). The dissociation was found to be mainly impulsive in nature with most of the available energy ($\sim 90\%$) released in translation. The angular distributions have also indicated the predominantly perpendicular nature of both the ground state and spin-orbit chlorine atom fragments. They found that the dominant transition in the A-band was due to the 1Q_1 state, which is in good agreement with our data [Fig. 2(a)].

While the main transition in the A-band of CH₃Cl is thought to be due to the 1Q_1 state [Fig. 2(a)], the 3Q_0 state becomes relevant for CH₃Br and dominant for CH₃I. The present DCS data in Fig. 2 show also that 1Q_1 is shifted to lower EEL energies when proceeding from CH₃Cl to CH₃Br to CH₃I. This observation is consistent with the data of Gedanken and Rowe,⁸ which provided qualitative support for the observed shift of the 1Q_1 MCD peak relative to the absorption peak. Moreover, this shift becomes more pronounced in methyl chloride because the absorption peak is almost entirely due to the 1Q_1 state so that with the increased intensity of the MCD positive signal for 3Q_0 , as you go along from CH₃I to CH₃Br to CH₃Cl, the negative MCD peak due to 1Q_1 is shifted to higher energies. The assumption of Townsend *et al.* that the energy ordering in the Franck–Condon region should be similar to the allowed transitions in CH₃I led them to conclude that at 6.42 eV (193 nm) the excitation is mainly due to the 1Q_1 surface.¹⁰ However this does not seem to be in total agreement with our data [see Fig. 2(a)], since the intensity of 1Q_1 at this energy loss (6.42 eV) is almost absent and the DCS value is too low. Instead, a transition to the 3Q_1 state seems more plausible which is reinforced in the EELS data at 30 eV incident energy and 20° scattering angle.

The electronic curve crossing *ab initio* study of CH₃Cl by Ajitha *et al.*⁹ showed that the slope of the repulsive state of the potential energy curves decreased in comparison to that for CH₃I. This has an effect on the broadened shape of the line profiles in the methyl chloride in respect to those due to other heavier halogens. As noted above the A-band here is mainly governed by the 1Q_1 transition [Fig. 2(a)], although we must also note that there is a non-negligible contribution

from the 3Q_0 state. Thus, a transfer of population through the conical intersection formed between the 1Q_1 and 3Q_0 surfaces must be significant in CH_3Cl .

D. CH_3F

The lowest excitation band in the methyl halides has in general been assigned to the well known *A*-band.²⁷ Figure 1(a), however, shows the EELS for CH_3F , where the lowest-lying excited electronic state is very broad and structureless. In fact this feature can also be assigned to the *B*-band,²⁴ with a vertical excitation energy of ~ 9.2 eV and it is due to the promotion of a fluorine lone pair to the $3s$ Rydberg series converging to the ionic electronic ground state.

The electronic excitation in CH_3F occurs from a molecular orbital with *e* symmetry, and so both the *B* and *C*-bands, as in the other heavier methyl halides, are also present.²⁴ Owing to the very weak spin-orbit coupling, that amounts to 0.01 eV (~ 100 cm^{-1}), which is far beyond our resolution, the splitting of these bands will be too small and the second component ($E_{1/2}$) very weak. A close inspection of Figs. 1(a)–1(d) reveals that the *A*-band in the methyl halides is progressively shifted towards higher energies as you go from I to Cl, so that in the particular case of methyl fluoride it must overlap and becomes indistinguishable from the *B*-band. Robin²⁷ has also noted that there is no distinct equivalent *A*-band in the case of methyl fluoride. Therefore, no further discussion will be made regarding the *Q* complex components for CH_3F .

Finally, we simply note that in our recent resonant vibrational excitation studies on methyl fluoride,² a strong indication for the resonant enhancement observed at about 6.6 eV, for the energy loss of 0.37 eV, was due to the formation of the 2A_1 shape resonance.² Since in the present EELS there is no evidence of such a contribution, we conclude that the lifetime of the resonance may strongly compete with autodetachment in these species.

IV. CONCLUSIONS

We have reported EELS and absolute DCSs for electron impact excitation of the halomethanes CH_3I , CH_3Br , and CH_3Cl in the *Q* complex of the *A*-band electronic states. This involved the excitation of the three 3Q_1 , 3Q_0 , and 1Q_1 states, in the order of increasing excitation energies $^3Q_1 < ^3Q_0 < ^1Q_1$, respectively. A transition to the steepest electronic excited potential energy curve, as was the case in CH_3I , led to dissociation in the *A*-band that contributed to a large broadening in its profile. The present electron spectroscopy data provided experimental evidence in support of earlier predictions from Mulliken⁷ and the MCD data of Gedanken and Rowe,⁸ as far as the role of the *Q* states in the *A*-band excitation of these methyl halides is concerned. Specifically the role of the 3Q_0 and 3Q_1 states becomes less significant as the mass of the halogen decreases. This effect is thought to be due to the weaker spin-orbit induced mixing with the 1Q_1 surface. Furthermore, distortion of the molecular frame upon excitation lowers the molecular symmetry from C_{3v} to C_s , resulting in considerable coupling between the 1Q_1 and 3Q_0 states. This is particularly relevant for CH_3I . This coupling

has been recognized as being due to a conical intersection that produces a considerable intersystem crossing as the molecules fall apart, therefore dictating the nature of the final products.

The transition intensities for the *A*-band of CH_3Cl , CH_3Br and CH_3I were all found to be a mixture of the parallel and perpendicular components 3Q_0 , 1Q_1 and 3Q_1 . For CH_3I the parallel transition to the 3Q_0 state prevails at 100 eV impact energies, with only minor contributions from the perpendicular 1Q_1 and 3Q_1 states. At 30 eV impact energy, on the other hand, the contributions of the 1Q_1 and 3Q_0 states to the *A*-band in methyl iodide are comparable. In CH_3Br the contributions from the 1Q_1 and 3Q_0 states are comparable and relatively independent of the impact energy. Finally, in CH_3Cl the 3Q_0 state becomes less relevant and the *A*-band is dominated by the 1Q_1 perpendicular transition at both impact energies. From a spectroscopic point of view the transition probabilities from the ground state to these excited states depends on both the electron impact energy and the electron scattering angle. Hence their corresponding spectral features are expected to emerge, specifically, under conditions more favorable for optically forbidden transitions at low energy electron impact. Notwithstanding that general comment, at both of the kinematics we investigated in methyl chloride, the transition to the 1Q_1 state dominates across almost the entire excitation band. This is in contrast to methyl bromide where comparable intensities for the 3Q_0 and 1Q_1 states are recorded under both conditions, whereas for CH_3I the 3Q_0 state is largely dominant only at the higher incident electron energy.

For CH_3Br , the electron spectroscopy data in the high-energy loss region were found to be dominated by the 1Q_1 state, whereas at low-energy loss it is dominated by the 3Q_1 state. Around 6.0 eV energy loss the majority of the fragments may be formed in the Br^* ($^2P_{1/2}$) channel. No effective crossing is observed between the 3Q_0 and 1Q_1 states here. For an electron incident energy of 100 eV, 5° scattering angle data for CH_3I and CH_3Cl at 5 and 7 eV energy loss, respectively, the majority of the fragments are also formed in the $^2P_{1/2}$ channel. However, this may change appreciably for low incident electron energy where strong competition between 1Q_1 state and 3Q_0 state occurs. Therefore the final dissociation channel can comprise both the ground ($^2P_{3/2}$) and the excited state ($^2P_{1/2}$) for the halogen (I and Cl).

ACKNOWLEDGMENTS

This work was conducted under the auspices of the Asia-Pacific Atomic Data Network as well as under the Japanese and Korean Collaborative Project of NIFS. H.K. gratefully acknowledges the award of both the JSPS and Sophia University Graduate Course Student Special Fellowships. P.L.-V. acknowledges his Visiting Professor position at Sophia University, Tokyo, Japan. This work forms part of the EU COST Actions CM0601 and CM0805 programmes “ECCL” and “The Chemical Cosmos,” respectively. Partial financial support from the ARC Centre of Excellence for Antimatter-Matter studies is also noted.

- ¹H. Kato, T. Asahina, H. Masui, M. Hoshino, H. Tanaka, H. Cho, O. Ingólfsson, F. Blanco, G. Garcia, S. J. Buckman, and M. J. Brunger, *J. Chem. Phys.* **132**, 074309 (2010).
- ²H. Kato, M. Hoshino, Y. Nagai, T. Tanaka, M. J. Brunger, O. Ingólfsson, and H. Tanaka, *J. Phys. B* **43**, 065205 (2010).
- ³B. R. Russell, L. O. Edwards, and J. W. Raymond, *J. Am. Chem. Soc.* **95**, 2129 (1973).
- ⁴S. Eden, P. Limão-Vieira, S. V. Hoffmann, and N. J. Mason, *Chem. Phys.* **331**, 232 (2007) and references therein.
- ⁵G. C. Causley and B. R. Russell, *J. Chem. Phys.* **62**, 848 (1975).
- ⁶D. Nachtigallova, D. E. Love, and K. D. Jordan, *J. Phys. Chem.* **100**, 5642 (1996).
- ⁷R. S. Mulliken, *J. Chem. Phys.* **8**, 382 (1940).
- ⁸A. Gedanken and M. D. Rowe, *Chem. Phys. Lett.* **34**, 39 (1975).
- ⁹D. Ajitha, M. Wierzbowska, R. Lindh, and P. A. Malmqvist, *J. Chem. Phys.* **121**, 5761 (2004).
- ¹⁰D. Townsend, S. K. Lee, and A. G. Suits, *J. Phys. Chem. A* **108**, 8106 (2004).
- ¹¹G. N. A. Van Veen, T. Baller, and A. E. De Vries, *Chem. Phys.* **92**, 59 (1985).
- ¹²Y. Amatatsu, K. Morokuma, and S. Yabushita, *J. Chem. Phys.* **94**, 4858 (1991).
- ¹³Y. Amatatsu, S. Yabushita, and K. Morokuma, *J. Chem. Phys.* **104**, 9783 (1996).
- ¹⁴A. Strobel, I. Fischer, A. Lochschmidt, K. Müller-Dethlefs, and V. E. Bondybey, *J. Phys. Chem. A* **98**, 2024 (1994).
- ¹⁵H. Tanaka, T. Ishikawa, T. Masai, T. Sagara, L. Boesten, M. Takekawa, Y. Itikawa, and M. Kimura, *Phys. Rev. A* **57**, 1798 (1998).
- ¹⁶J. N. H. Brunt, G. C. King, and F. H. Read, *J. Phys. B* **10**, 1289 (1977).
- ¹⁷R. E. Kennerly, *Phys. Rev. A* **21**, 1876 (1980).
- ¹⁸S. Trajmar, J. M. Ratliff, G. Csanak, and D. C. Cartwright, *Z. Phys. D: At., Mol. Clusters* **22**, 457 (1992).
- ¹⁹D. V. Fursa and I. Bray, *Phys. Rev. A* **52**, 1279 (1995).
- ²⁰M. Lange, J. Matsumoto, J. Lower, S. Buckman, O. Zatsarinny, K. Bartschat, I. Bray, and D. Fursa, *J. Phys. B* **39**, 4179 (2006).
- ²¹S. K. Srivastava, A. Chutjian, and S. Trajmar, *J. Chem. Phys.* **63**, 2659 (1975).
- ²²L. Boesten and H. Tanaka, *At. Data Nucl. Data Tables* **52**, 25 (1992).
- ²³T. N. Olney, G. Cooper, W. F. Chan, G. R. Burton, C. E. Brion, and K. H. Tan, *Chem. Phys.* **205**, 421 (1996).
- ²⁴T. N. Olney, G. Cooper, W. Chan, G. R. Burton, C. E. Brion, and K. H. Tan, *Chem. Phys.* **218**, 127 (1997).
- ²⁵T. N. Olney, G. Cooper, and C. E. Brion, *Chem. Phys.* **232**, 211 (1998).
- ²⁶T. N. Olney, G. Cooper, W. F. Chan, G. R. Burton, C. E. Brion, and K. H. Tan, *Chem. Phys.* **189**, 733 (1994).
- ²⁷M. B. Robin, *Higher Excited States of Polyatomic Molecules* (Academic, New York, 1974), Vol. I.
- ²⁸B. R. Johnson and J. L. Kinsey, *J. Phys. Chem.* **100**, 18937 (1996).
- ²⁹K. Q. Lao, M. D. Person, P. Xayariboun, and L. J. Butler, *J. Chem. Phys.* **92**, 823 (1990).
- ³⁰C. Escure, T. Leininger, and B. Lepetit, *J. Chem. Phys.* **130**, 244305 (2009).